Lazareva, Olesya ; Druschel, Gregory ; Pichler, Thomas

Understanding arsenic behavior in carbonate aquifers: Implications for aquifer storage and recovery (ASR)

Journal Article	as:	peer-reviewed accepted version (Postprint)
DOI of this document*(secondary publication):		https://doi.org/10.26092/elib/3221
Publication date of this document:		15/08/2024

* for better findability or for reliable citation

Recommended Citation (primary publication/Version of Record) incl. DOI:

Olesya Lazareva, Gregory Druschel, Thomas Pichler, Understanding arsenic behavior in carbonate aquifers Implications for aquifer storage and recovery (ASR), Applied Geochemistry, Volume 52, 2015, Pages 57-66, ISSN 0883-2927, https://doi.org/10.1016/j.apgeochem.2014.11.006.

Understanding arsenic behavior in carbonate aquifers: Implications for aquifer storage and recovery (ASR)

Olesya Lazareva [a,*], Gregory Druschel [b], Thomas Pichler [c]

[a] University of Delaware Environmental Institute, Newark, DE, USA
[b] Department of Earth Sciences, Indiana University-Purdue University, Indianapolis, IN, USA
[c] FB 5 Geosciences, University of Bremen, 28359 Bremen, Germany

1. Introduction

Aquifer storage and recovery (ASR) is the storage of treated surplus surface water in a confined aquifer followed by its recovery during times of need. The ASR procedure has been widely implemented around the world to meet increasing water demand and to provide a more sustainable alternative to extensive groundwater consumption (Alley et al., 1999). However, perturbations of the physicochemical conditions during ASR in Florida, Australia, Denmark, and the Netherlands caused elevated arsenic (As) concentrations in recovered water (Arthur et al., 2005; Jones and Pichler, 2007; Mirecki et al., 2012; Mirecki, 2006; Stuyfzand, 1998; Stuyfzand and Timmer, 1999; Vanderzalm et al., 2007).

In Florida, ASR is currently being widely implemented, but elevated As concentrations of up to 130 μg/L in recovered water (Arthur et al., 2002; Arthur et al., 2005; Williams et al., 2002) exceeded the As drinking water standard of 10 μg/L (EPA, 2009), making permitting more complex. The storage zone for ASR is generally the Upper Floridan Aquifer (UFA), a regional carbonate aquifer system. Arsenic in the aquifer matrix is of geogenic origin and mostly associated with pyrite (Lazareva and Pichler, 2007; Price and Pichler, 2006). Arsenic concentrations in pyrite from the Avon Park Formation (APF) and Suwannee Limestone which include the Upper Floridan Aquifer, and the Hawthorn Group, which in part includes the Intermediate Aquifer were reported as high as 5820, 11,200 and 8260 mg/kg, respectively (Lazareva and Pichler, 2007; Price and Pichler, 2006; Pichler et al., 2011). Consensus is that the injection of oxygenated surface waters into reducing native groundwater during ASR operations causes oxidative dissolution of pyrite, and thus the release of As to the stored water (Arthur et al., 2002; Arthur et al., 2005).

The objective of this investigation was to carry out a series of column bench-scale leaching experiments at different redox conditions using rock cuttings from the APF to identify important reactions that control water quality changes during ASR cycle testing and incorporate those results into fully coupled reactive transport models using the computer code Geochemist's Workbench (Bethke, 1998; Bethke, 2006a, 2006b). The goal was to gain a better understanding of As mobilization from pyrite bearing limestone aquifers at a much finer scale than previous modeling efforts (Saunders et al., 2008; Wallis et al., 2011).

* Corresponding author. Tel.: +1 (302) 831 0608; fax: +1 (302) 831 0605.
E-mail address: olazarev@udel.edu (O. Lazareva).

2. Methods

2.1. Experimental setup

The leaching experiments were performed in standing PVC columns of 0.019 m in diameter, and 0.3 m and 0.5 m in length, which were filled with rock cuttings from the Avon Park Formation (APF) that were collected during installation of a well in Polk County (central Florida) (Pichler et al., 2011) and represented the interval from 255 m to 257 m. Until time of preparation and chemical analysis the cuttings were stored in a 5 L bucket under a N_2 atmosphere. Prior to packing the columns, the rock cuttings were dried and ground using agate grinder to a size of coarse sand to increase the surface area. The cuttings were examined by hand lens, stereo microscope and scanning electron microscope (SEM) for the possibility of post-drilling oxidation of pyrite. Two random samples and 2 "targeted" samples were collected for the determination of chemical composition. The two "targeted" samples represented cuttings, which were deemed to have higher As, based on clay or pyrite content, following the reported procedures (Pichler et al., 2011; Price and Pichler, 2006). To characterize mineral phases, the samples were examined with a Hitachi S-3500N SEM-EDS instrument. To determine bulk rock chemical composition the samples were digested in 3:1 mixture of HCl and HNO_3 following established procedures (Lazareva and Pichler, 2007; Price and Pichler, 2006). Calcium, Fe, Mg, Mn, Na, K, S, P, Si and Al were determined by inductively coupled plasma – optical emission spectrometry (ICP–OES) and As by hydride generation – atomic fluorescence spectrometry (HG–AFS) (Table S1).

To simulate ASR injectate, the City of Tampa drinking water was used as an analog and collected from a tap in the laboratory after extensive flushing. Mandated by Federal regulation, the ASR injectate has to be treated to meet primary and secondary drinking water standards and requirements (CFR). Thus, ASR injectate and drinking water in central Florida, specifically the City of Tampa, undergo the same treatments including UV disinfection, chlorination or ozonation, and therefore are close with respect to chemical composition, pH, temperature (T) and dissolved oxygen (DO) content. Native Floridan groundwater (GW) was collected from an Upper Floridan Aquifer well located on the USF Tampa campus (Table S3). The water was collected into a 9.5 L amber carboy equipped with quick disconnect closures. To minimize atmospheric contact prior to sampling the carboy was flushed and filled with N_2. During collection N_2 was replaced with groundwater, thus ensuring an oxygen-free atmosphere. The groundwater and injectate water were immediately analyzed for pH, T, ORP (oxidation–reduction potential), DO, H_2S, and Fe^{2+}. A CHEMets Colorimetric field kit was used for Fe^{2+} analysis and H_2S was analyzed using the Methylene Blue Method on a HACH DR 2400 photospectrometer. The water samples were filtered through a 0.45 μm membrane for the determination of major anions by ion chromatography (IC), major cations by ICP–OES and As by HG–AFS.

After packing, the columns were flushed with N_2 gas for about 24 h to eliminate any O_2 present in the pore space. The water was percolated through the columns from the bottom up, thus allowing for a more uniform flow through the columns and complete saturation of the rock. To achieve a flow rate of about 2 mL/min and to avoid any contact with atmospheric oxygen, Watson-Marlow multichannel peristaltic pumps were used. The leachate samples were collected from the top of the columns at certain intervals (every 60 mL) and analyzed for physical and chemical parameters following the procedures described above. The column porosity was determined as the ratio of the weight of water filling the column to the total weight of water and sediment in the column, subtracting the weight of the column as n = mass (water)/(mass (water + sediment)) ∗ 100% (Table S2).

Table 1
Reactions and reaction rate constants used for construction of the reactive transport model (T = 22.3 °C).

Reactions	log K
Minerals (reactants)	
Calcite: $CaCO_3 + H^+ = Ca^{++} + HCO_3^-$	1.7492
Dolomite: $CaMgCO_3 + 2\ H^+ = Ca^{++} + Mg^{++} + 2\ HCO_3^-$	2.6096
Pyrite: $FeS_2 + H_2O + 3.5\ O_2(aq) = Fe^{++} + 2\ H^+ + 2\ SO_4^{--}$	219.6902
Arsenopyrite: $AsFeS + 2.5\ H_2O + 0.375\ SO_4^{--} + 0.375\ H^+ = Fe^{++} + As(OH)_4^- + 1.375\ HS^-$	188.1095
Gypsum: $CaSO_4{:}2\ H_2O = 2\ H_2O + Ca^{++} + SO_4^{--}$	−4.4505
Surface species	
$>(w)FeH_2AsO_3 + 2\ H_2O = H^+ + As(OH)_4^- + >(w)FeOH$	−14.6852
$>(w)FeH_2AsO_4 + 2\ H_2O = H^+ + 0.5\ O_2(aq) + As(OH)_4^- + >(w)FeOH$	−41.7508
$>(w)FeHAsO_4^- + 2\ H_2O = 0.5\ O_2(aq) + As(OH)_4^- + >(w)FeOH$	−35.9508
$>(w)FeOHAsO_4^{--} + H_2O + 2\ H^+ = 0.5\ O_2(aq) + As(OH)_4^- + >(w)FeOH$	−23.0208

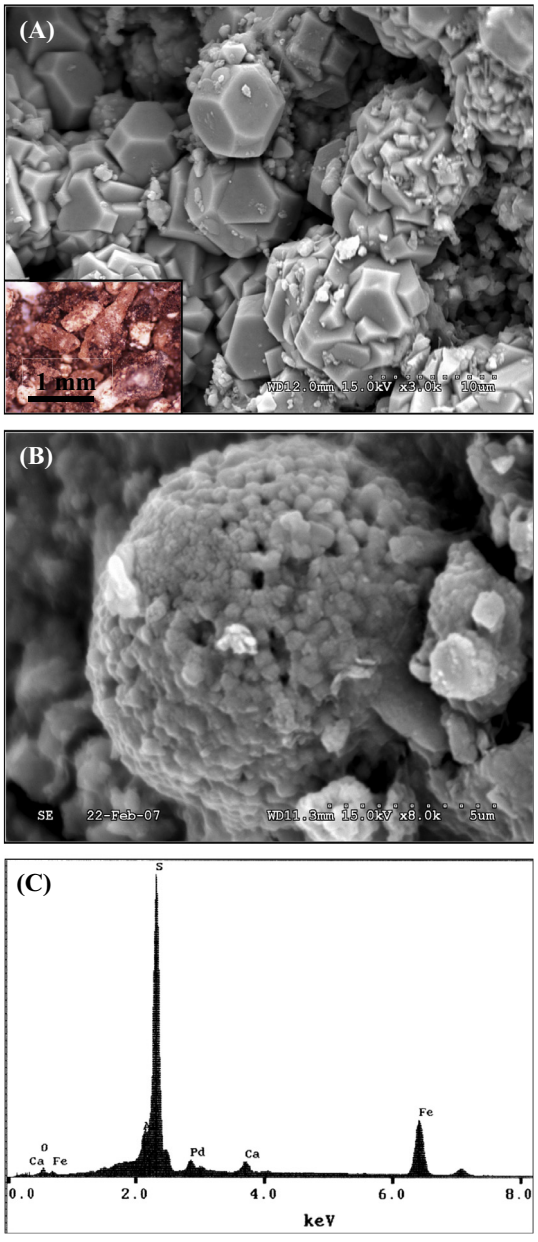

Fig. 1. Photomicrograph (left corner A), scanning electron micrographs of dodecahedral (A) and framboidal (B) pyrites in the Avon Park Formation and EDX spectrum (C). Note: Bar scales in lower right are 10 μm and 5 μm.

2.2. Geochemical modeling

The chemical reactions and chemical evolution of the aqueous phase were modeled using the Geochemist's Workbench (GWB) Professional modeling platform (version 6.0.5) including the React and X1t modules (Bethke, 2006a,b). The React program calculates the equilibrium states in solution, the state of mineral saturation, as well as the fugacity of dissolved gases (Bethke, 2006a). It can consider a number of mineral interactions such as sorption and ion exchange, plus kinetic constrains on reactions and mixing. At the same time, X1t constructs a 1D reactive flow and transport model which is coupled to the React code (Bethke, 2006b). Redox equilibrium of the system is the default state for most thermodynamic modeling software including GWB – the assumption that all redox couples are in equilibrium with each other. The program allows "decoupling", which is the removal of specific redox couples from this assumption to model in limited way true redox disequilibrium.

Setup of the models was based on the bulk rock composition, the rock mass for a 0.5 m column and the water chemistry analyses described above. Due to the complexity of the carbonate system during water–rock interaction in the columns, such as the progressive transformation of the solution and mineral saturation states, four geochemical models were developed, which represent the theoretical extremes of column experiments in an open or closed system:

- Titration model (1) simulated introduction of surface (injectate) water into an aquifer under closed system conditions. This model titrated the minerals listed in Table S4 into 60 ml of water (composition in Tables S1 and S3) in 100 increments where the amount of oxygen was limited to the amount dissolved in the initial water.
- Titration model (2) simulated introduction of injectate water into an aquifer under open system conditions. This model titrated the minerals listed in Table S5 into 60 ml of water (composition in Tables S1 and S3) in 100 increments where the amount of oxygen was unlimited ($O_{2(aq)}$ constrained by equilibrium with unchanging atmospheric $O_{2(g)}$).
- Titration model (3) simulated introduction of injectate water into an aquifer in the presence of considerable abundance of pyrite and arsenopyrite under open system conditions. This model is identical to model (2) excepting that a higher mass of minerals was used (Table S6).
- Flow-through 1D reactive transport model (4) simulated the column leaching experiments. Model parameters for this model are fundamentally different from models (1) to (3) (but the water composition and minerals are similar) and meant to model the conditions of the column experiment in more detail by including flow through a simple column of 10 compartments, or nodes to simulate how key reactions are behaving across the column in time as water flows through it (Table S7).

The simulation was set for 340 min and the volume of reacting fluid was 60 mL to reflect the conditions of the leaching experiments. The simulation was designed based on the input flow rate so the model is still in steps related to volume, but converted to time based on a flow rate. During the geochemical modeling, mineral precipitation, dissolution and sorption were included in the reaction network (Dzombak and Morel, 1990; Wolery et al., 1994). The surface complexation modeling the FeOH.dat database (Dzombak and Morel, 1990) was implemented to account for As sorption onto hydrous ferric oxides (HFO). It included the surface complexation constants, surface site density, and the specific surface area of the HFO species (Dzombak and Morel, 1990).

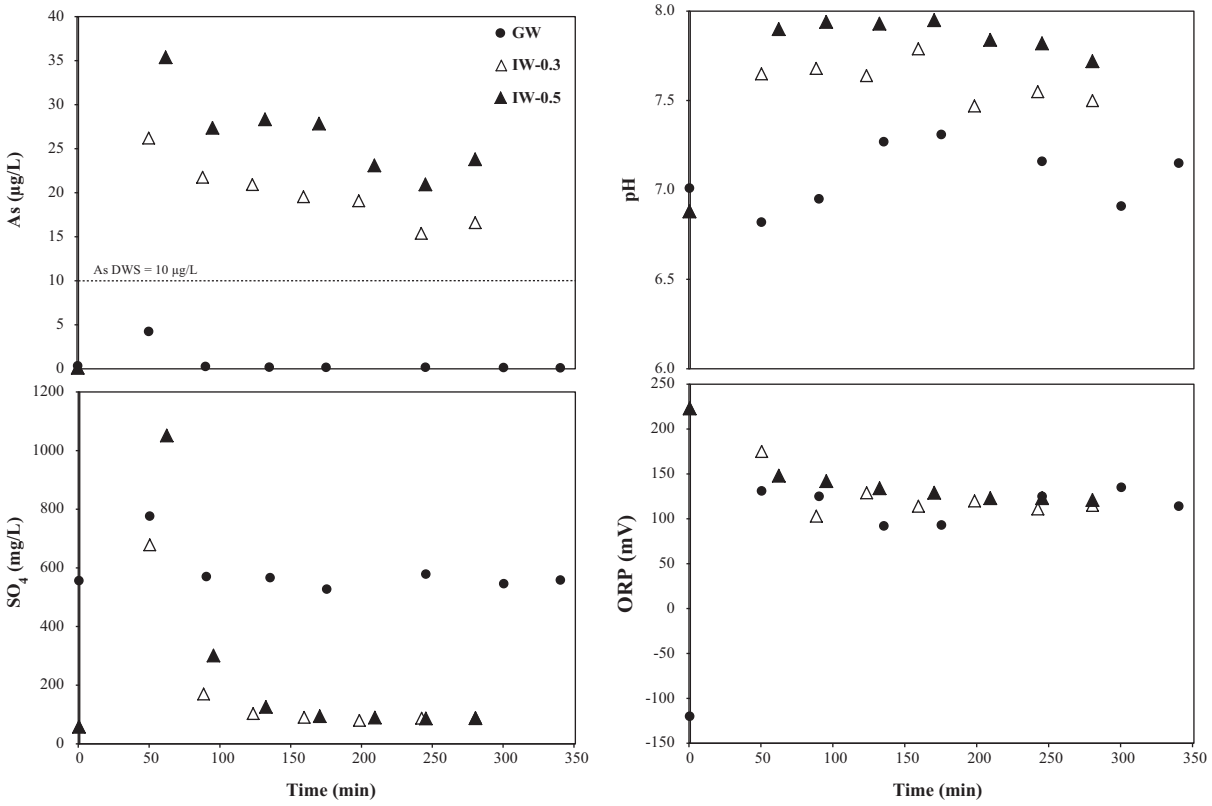

Fig. 2. As, SO_4, pH, and oxidation–reduction potential (ORP) over time in leachates recovered from the Avon Park Formation (255 m to 257 m). Note: GW: groundwater (0.3 m column); IW-0.3: injectate water (0.3 m column); IW-0.5: injectate water (0.5 m column); each point represents 60 mL of sample pore volume; values for the initial water are plotted on the *Y*-axis.

Table 1 shows reactions and equilibrium constants used in the four models.

Prior to the simulations, thermodynamic data for arsenopyrite (AsFeS) in the thermo.dat database (Wolery et al., 1994) was modified to switch the controlling redox couple for the mineral to the redox couple HS^-/SO_4^{2-} instead of $AsH_3(aq)/As(OH)_4^-$. The dissolution reaction of arsenopyrite was modified from (1) to (2):

$$AsFeS + 2H_2O + 0.5H^+ = Fe^{++} + 0.5As(OH)_4^- + 0.5AsH_3 + HS^- \quad (1)$$

$$AsFeS + 2.5H_2O + 0.375H^+ + 0.375SO_4^{--} = Fe^{++} + As(OH)_4^- + 1.375HS^- \quad (2)$$

Redefining arsenopyrite was necessary for two reasons: (1) to put the arsenopyrite dissolution reaction in the same terms as the pyrite dissolution reaction and (2) to put the definition of redox state for this mineral dissolution in terms of S speciation rather than As speciation. This allowed modeling of geogenic As in pyrite as a combination of pyrite and arsenopyrite. This combination considers only the free energy changes in the As–S solid solution as a simple mechanical mixing of the two end-members, but nevertheless should provide a reasonable thermodynamic starting point.

3. Results and discussion

3.1. Rock chemical composition

Results from the geochemical and mineralogical analysis of the 255–257 m interval corresponded to previous studies of the APF (Miller, 1986; Pichler et al., 2011; Scott, 1992). The APF rock cuttings used in the column experiments consisted of a limestone – dolostone matrix with minor mineral phases, such as pyrite, dark brown clays and gypsum (Table S1). Commonly, the dark brown dolostone was highly fractured and sucrosic in texture. The SEM analysis confirmed the presence of dodecahedral and framboidal pyrite crystals with unoxidized surfaces (Fig. 1). Bulk rock chemical compositions are presented in Table S1. The concentration of As varied from 3.7 mg/kg to 5.2 mg/kg with average value of 4.7 mg/kg. The amount of FeS_2 varied from 0.11 wt.% to 0.04 wt.% with the average value of 0.08 wt.%. It was calculated from the bulk Fe concentration due to the presence of gypsum. The average As/FeS_2 molar ratio was 0.01.

3.2. Leaching experiments

During the experiments, groundwater (GW) was injected into a 0.3 m column and injectate water (IW) was injected into 0.3 m and 0.5 m columns to compare As leaching patterns. The columns contained between 162 g and 304 g of sediment with an average

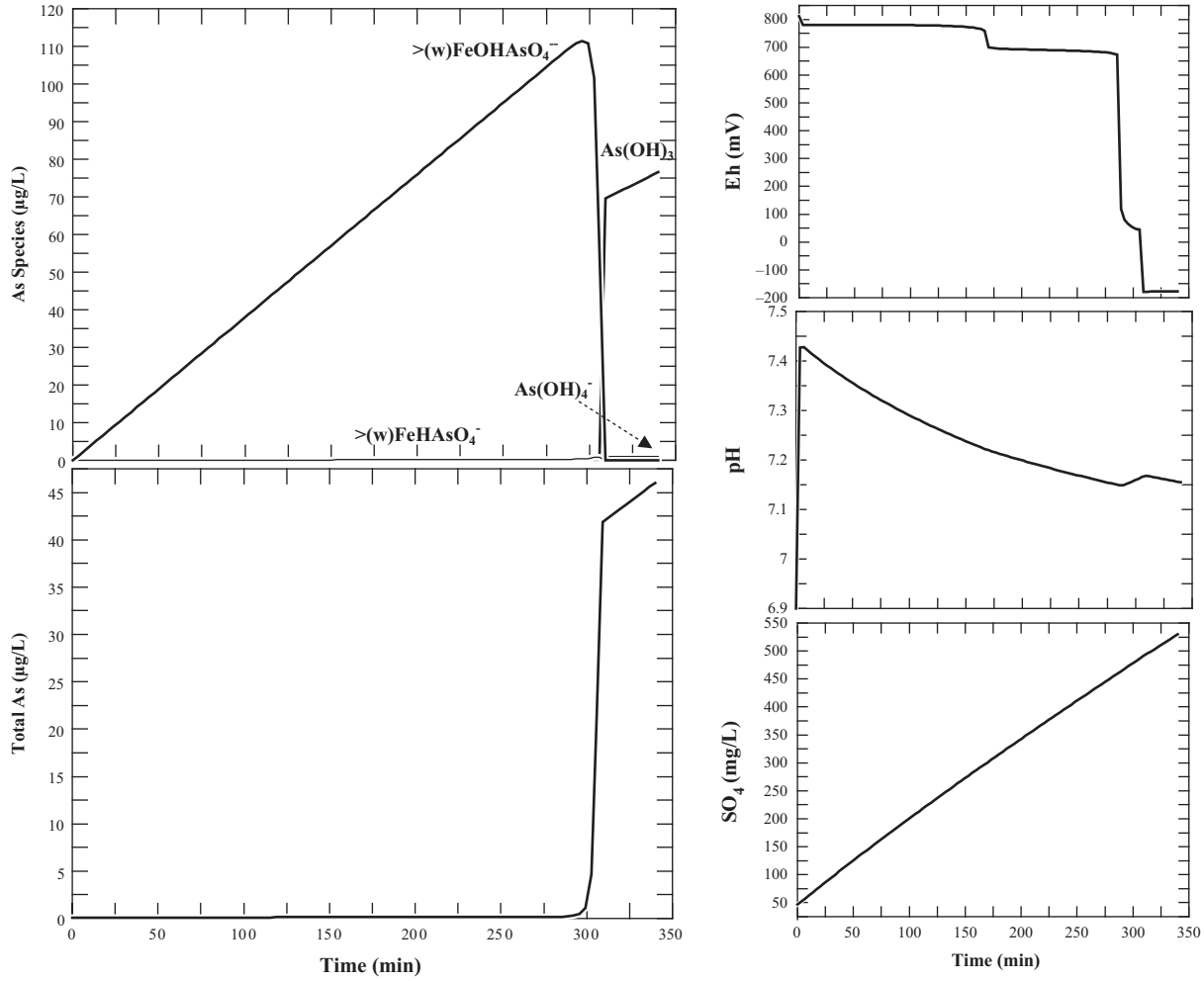

Fig. 3. Modeled distribution of As species, total As, Eh, pH, and SO_4 over time (Model 1: water–rock interaction between the aquifer matrix and surface water – Closed System).

porosity of 14.6% (Table S2). All experiments were performed for about 5 h (280–340 min) and resulted in the recovery of 420 mL of leachate from each column (Fig. 2, Table S3).

Injection of GW mobilized As at concentrations up to 4.3 μg/L in the first pore volume. Arsenic concentrations subsequently declined to <0.1 μg/L at the end of experiment (Fig. 2). The first peak of As could be due to a possible micro-oxidation of pyrite surfaces along the fractures and crystal borders prior to the experiment and the formation of a thin film of ferrous sulfate phases such as szomolnokite ($FeSO_4{\cdot}H_2O$) or schwertmannite ($Fe_8O_8(OH)_6SO_4$) with incorporation of As into these structures (Costagliola et al., 1997; Pratesi and Cipriani, 2000). Therefore, the injection of anoxic groundwater could facilitate a minute release of As associated with a ferrous sulfate phase. Consistent with this idea, a previous study of As abundance in the Suwannee Limestone of the Upper Floridan Aquifer showed enrichment of As along the rim of framboidal pyrite (Price and Pichler, 2006).

The introduction of oxygen- and nitrate-rich surface (Jagucki et al., 2009) IW into 0.3 m and 0.5 m columns showed that As concentrations in the first pore volume were up to 26.2 μg/L and 35.4 μg/L, respectively (Fig. 2). These values were higher than the current As drinking water standard of 10 μg/L (EPA, 2009). The concentration of SO_4 increased by more than one order of magnitude from 58 mg/L to 679 mg/L and 1051.2 mg/L, respectively. The pH values increased from 6.9 to 7.7 and 7.9, while the oxidation–reduction potential (ORP) declined from 223 mV to about 115 mV and 121 mV, respectively, due to consumption of oxygen by pyrite oxidation. After 280 min of injection, the concentration of As in leachates decreased to 16.6 μg/L and 23.8 μg/L for 0.3.m and 0.5 m columns, respectively.

Pyrite is not stable under oxidizing conditions whereas $Fe(OH)_3$ is not stable under reducing subsurface conditions (Evangelou, 1995). Generally, the oxidation and dissolution of pyrite by O_2 acts as a source for acidity, sulfate, iron and arsenic, and is a three step process:

(1) $FeAs_xS_{2-x} + 7/2O_2 + H_2O \rightarrow Fe^{2+} + (2-x)SO_4^{2-} + xAsO_4^{3-} + 2H^+$

Fe^{2+}can be further oxidized to Fe^{3+}, which precipitates as HFO (displayed as $Fe(OH)_3$):

(1) $Fe^{2+} + 1/4O_2 + H^+ \rightarrow Fe^{3+} + 1/2H_2O$ and
(2) $Fe^{3+} + 3H_2O \rightarrow Fe(OH)_3 + 3H^+$

The breakthrough curves for As and SO_4 in the leachates showed initially high concentrations for these species followed by a rapid decline before reaching almost steady-state conditions of mineral dissolution after about 3 h (Fig. 2). During experimental oxidation of arsenopyrite, a similar sudden reduction of As and S release rates occurred in the first 15 h (Walker et al., 2006) and were interpreted as limited surface oxidation and preferential reactions on fractured mineral surfaces (Borda et al., 2004). The

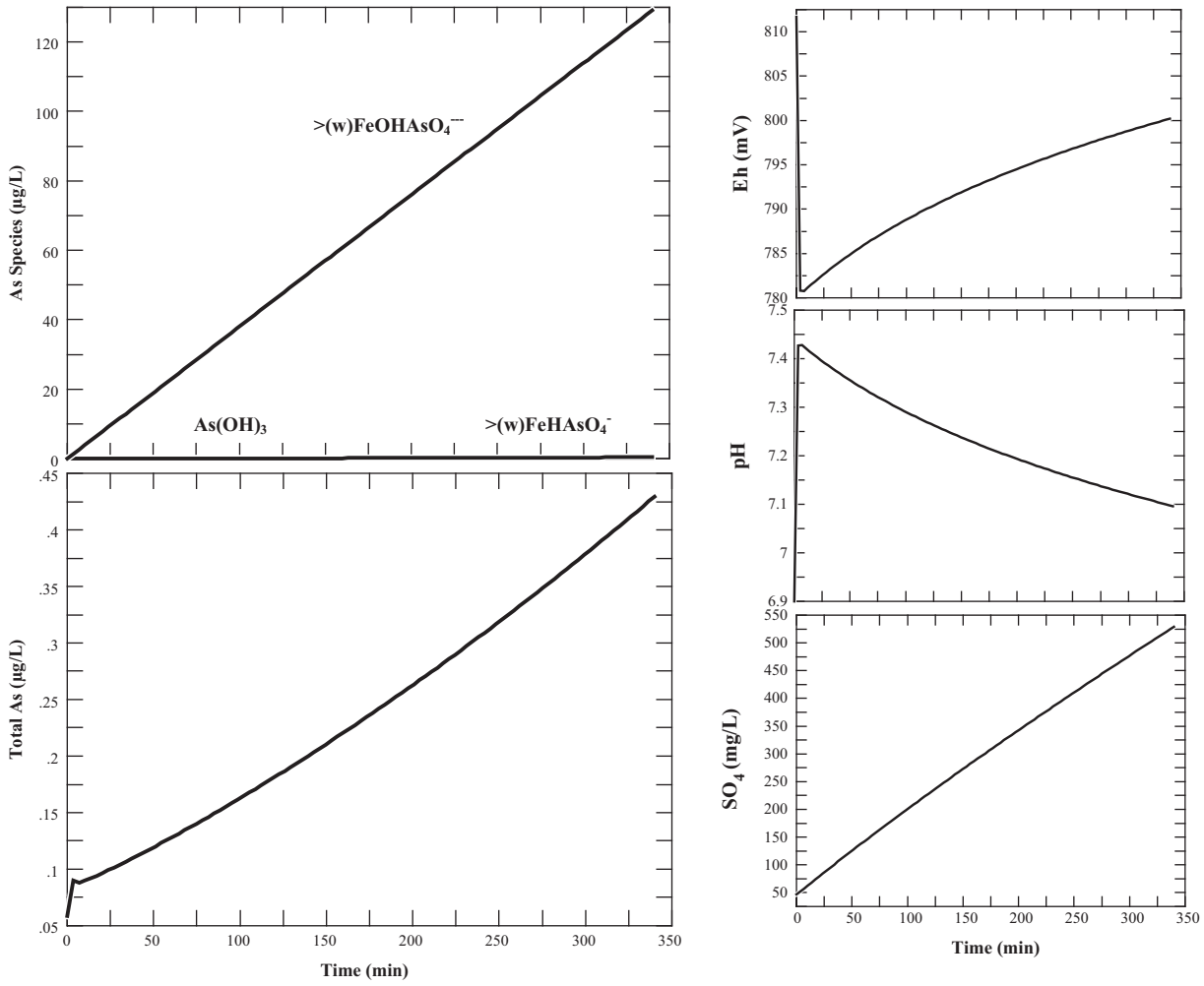

Fig. 4. Modeled distribution of As species, total As, Eh, pH, and SO_4 over time (Model 2: water–rock interaction between the aquifer matrix and surface water – Open System).

increase in SO_4 can be explained by (a) the oxidative dissolution of pyrite or (b) the dissolution of anhydrite/gypsum. Since the Ca concentration did not increase significantly at the same time as SO_4, the dissolution of anhydrite/gypsum can be ruled out as a significant source for SO_4. This leaves the oxidative dissolution of pyrite to explain the observed increase in SO_4 according to Eq. (1). Taking into consideration the molar ratio of Fe and S in pyrite (1:2), the Fe concentration in the leachate should have increased as well. However, the concentration of Fe in leachates was substantially lower or even undetectable, which indicates that Fe was retained in the column, most likely due to the precipitation of HFO. Due to the high sorption capacity of HFO, the released As should have been adsorbed onto neo-formed HFO and thus retained in the column (Bowell, 1994; Chao and Theobald, 1976; Evangelou, 1995; Inskeep et al., 2002; Hinkle and Polette, 1999; Hongshao and Stanforth, 2001; Manning and Goldberg, 1998; Nickson et al., 2000; Pichler et al., 1999; Vanderzalm et al., 2011). HFO is stable only in oxic to suboxic conditions (ORP < −200 mV) which typically are not represented in the confined Upper Floridan Aquifer. It is possible that if As was released from an oxide or sulfate salt coating on the pyrite grains in the column on initial wetting with the fluid, that As would have been transported through the column before HFO mineral formation and subsequent As sorption would limit it's mobility. This would explain the initial spike in As and SO_4^{2-} coming out of the column, consistent with experimental studies of pyrite and arsenopyrite oxidation (Moses et al., 1987; Walker et al., 2006). The results of the column experiments agree with field experiments in the Netherlands (Wallis et al., 2010) showing the initial As peak during injection due to the dissolution of arsenopyrite, which diminishes quickly due to increased availability of HFO, transformation of As(III) to As(V), and As adsorption on freshly precipitated $Fe(OH)_3$.

3.3. Geochemical modeling

The aim of the modeling effort was to investigate the key geochemical processes and test the conceptual models on As release during the leaching experiments, assuming four different scenarios. The parameters for each model are listed in Tables S4–S7.

3.3.1. Water–rock interaction between the aquifer matrix and surface water (Closed System)

The goal of this model was to describe the reaction between the aquifer matrix and surface (injectate) water under closed system conditions using the React code. This model did not consider flow and there was no source of atmospheric O_2 to replenish O_2 in the fluid. Based on the results from the bulk rock chemical analysis (Table S1), the aquifer matrix in the model was represented by 248 g of calcite ($CaCO_3$), 30 g of dolomite ($CaMgCO_3$), 25 g of gypsum ($CaSO_4$), 0.2 g of pyrite (FeS_2), and 0.002 g of arsenopyrite (AsFeS) (Table S4), according to the 0.01 As/FeS_2 molar ratio.

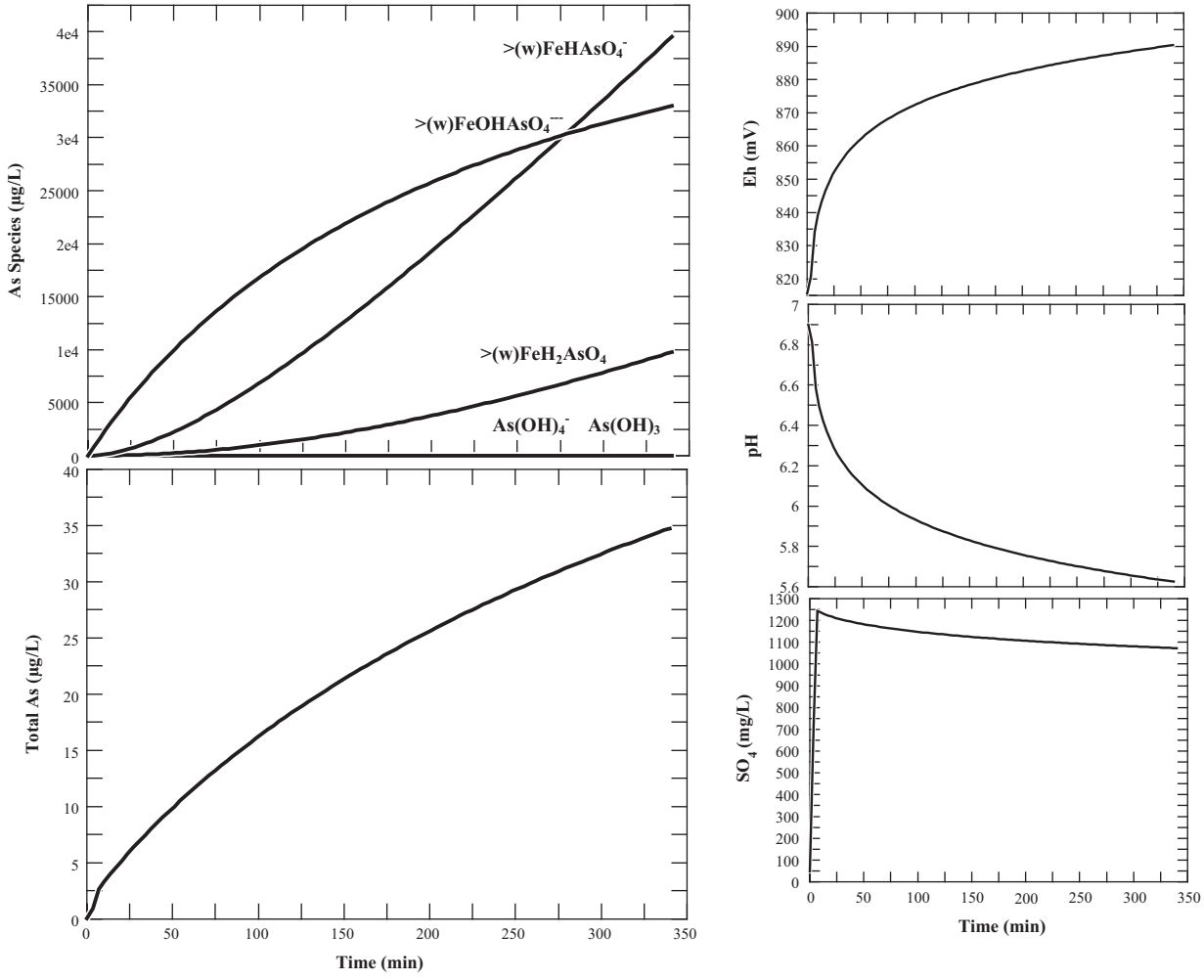

Fig. 5. Modeled distribution of As species, total As, Eh, pH, and SO4 over time (Model 3: water–rock interaction between the aquifer matrix and surface water – Open System, higher amount of As).

The geochemical modeling showed that about 6×10^{-4} g of pyrite and 6×10^{-6} g of arsenopyrite per total mass rock were dissolved over 340 min. The increasing concentration of Ca^{2+} indicated the dissolution of limestone during water–rock interactions (data not shown). The redox conditions remained oxidizing for about 300 min after which they sharply changed to reducing (Fig. 3). The Eh decreased from +800 mV to −160 mV; in the model this switch to reducing conditions was caused by the depletion of oxygen and thus, a change from oxidative sulfide mineral dissolution to redox equilibrium between the remaining sulfide minerals and the water phase. The pH of the system increased from 6.9 to 7.15 in the effluent (Fig. 3). The concentration of SO_4 increased from about 50 mg/L to 530 mg/L. About 110 μg/L of As was sorbed onto HFO via weak bonding ($FeOHAsO_4^{2-}$) until 300 min into the simulation, when the As was released back to solution as $As(OH)_3$ through the reductive dissolution of HFO. During that time, the system was saturated with respect to pyrite and arsenopyrite. The concentration of total As in the leachate was well below drinking water standard until after the sudden change in redox state, when it went up to 45 μg/L (Fig. 3).

3.3.2. Water–rock interaction between the aquifer matrix and surface water (Open System)

The goal of this model was to describe the reaction between the aquifer matrix and injectate water under open system conditions, i.e. the amount of O_2 in the system was fixed and thus, did not decrease as the reaction progressed. This step was important to evaluate how much pyrite could react and the amount of As, which could be leached from the aquifer matrix, if O_2 was not limited and the system remained oxic. The composition of the aquifer matrix was unchanged from the previous model (Table S5).

This geochemical model demonstrated that similarly to model (1) about 6×10^{-4} g of pyrite and 6×10^{-6} g of arsenopyrite were dissolved over 340 min. In contrast to the previous model (1), HFO remained stable and Eh remained positive (Fig. 4). The pH of the system changed from 6.9 to 7.1 in the effluent. The concentration of SO_4 increased from about 50 mg/L to 530 mg/L. Although approximately the same amount of pyrite and arsenopyrite reacted during the simulations, the concentration of total As in the fluid only reached 0.4 μg/L at the end of the simulation (Fig. 4). About 128 μg/L of As was sorbed onto HFO via weak bonding ($FeOHAsO_4^{2-}$ and $FeHAsO_4^{-}$). Thus, maintaining oxic condition in this system keeps neo-formed HFO stable and limits As release to the water phase; this process is likely not representative of how significant As is mobilized in subsurface carbonate aquifers since the dissolved oxygen that is recharged in the Floridan Aquifer is reduced very quickly (about 24-h half-life) (Mirecki et al., 2012).

3.3.3. Water–rock interaction between the aquifer matrix and surface water (Open System; higher amount of As)

The major goal of the model (3) was to describe the water–rock interaction of the system that would release the amount of As

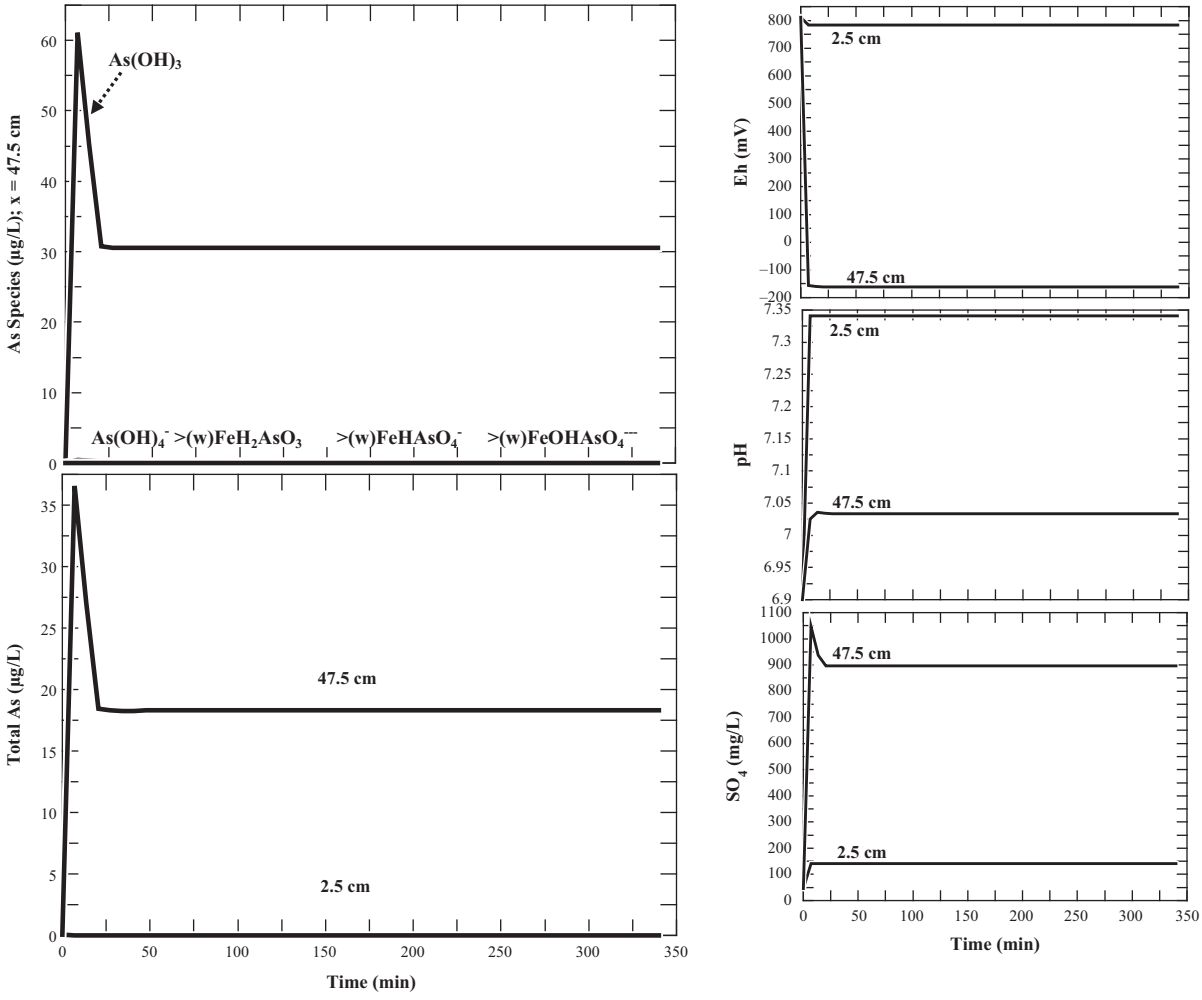

Fig. 6. Modeled distribution of As species, total As, Eh, pH, and SO_4 over time (Model 4: 1D reaction-transport model of water–rock interaction between the aquifer matrix and surface water).

observed in experiments and in the field through only pyrite/arsenopyrite oxidation in an open system (fixed source of O_2). Thus, the aquifer matrix was unchanged to previous examples except for the amount of pyrite (FeS_2) and arsenopyrite (AsFeS), which was modified to 0.4 g and 0.004 g, respectively, to ensure sufficient sulfide material available for the model (Table S6).

During the simulations, the Eh of the system remained positive indicating an oxidizing environment (Fig. 5). The pH dropped from 6.9 to 5.6 contradicting the experimental data (Figs. 2 and 5). The concentration of SO_4 steeply increased within 15 min of simulation from about 50 mg/L to 1250 mg/L. The concentration of total As in the fluid did get up to 35 μg/L, similar to the experimental data (Fig. 2), with a much larger quantity of As adsorbed onto HFO. In order to achieve this amount of As in solution, 0.4 g of pyrite and 0.004 g of arsenopyrite needed to be dissolved from the column and the amount of As released remained in equilibrium with the HFO generated. According to the bulk rock chemical analysis, the samples from the APF contained about 800 mg/kg of pyrite or 0.2 g in the 0.5 m column (Table S1). This simulation suggests that the brute force method of generating high-arsenic waters in completely oxidized settings for ASR systems would require much more sulfide material than is generally available in the aquifer matrix, and would yield higher sulfate and lower pH than is typically measured. Coupled with the results of model (2), oxidizing conditions may initiate As release from sulfide minerals, but the key to aqueous As release in ASR systems lies with the stability and As sorption capacity of HFO. This confirms the broader assumptions of several studies about As mobility at other localities worldwide (Stuyfzand, 1998; Stuyfzand and Timmer, 1999; Vanderzalm et al., 2007; Wallis et al., 2010), including southwestern Florida (Wallis et al., 2011).

3.3.4. 1D reaction-transport model of water–rock interaction between the aquifer matrix and surface water

The X1t code was used to model reactive transport in one dimension (Bethke, 2006b) to simulate the geochemical and hydrodynamic conditions in the column experiments (Fig. 2). This model was important to investigate the results of bench-scale experiments in time and space and to evaluate the key geochemical processes occurring along the flow path. This is one step further than the column experiments, which allowed only the observation of one point in time, i.e., at the column exit. Based on that one observation point, chemical reactions along the flow path in the column had to be inferred.

The transport model was constructed with the same solution and solid phase compositions as in models (1) and (2). The dimensions of the simulated column were 50 cm (length) by 2 cm (width). Consistent with the leaching experiments, the discharge rate of fluid in the column was 0.01 cm^3/cm^2 sec, and the porosity was 15 % (Table S7).

Based on the observed sensitivity during the three titration models the amounts of FeS_2 and AsFeS were changed to 0.2 g and 0.0007 g, respectively, to adjust this model with the experimental data output (Table S7). This geochemical modeling showed that about 8×10^{-5} g/cm^3 of pyrite and 2.9×10^{-7} g/cm^3 of arsenopyrite were dissolved at the end of the column over 340 min.

The pH of the system varied from 6.9 (initial fluid) to 7.0 at the end of the column. At the same time the highest pH of 7.3 was reached at 2.5 cm distance along the flow path. The concentration of total As in the leachate reached up to 36 μg/L and the concentration of SO_4 increased from 47 mg/L to 1046 mg/L at the end of the column. The Eh of the system changed rapidly from oxidizing to reducing (+800 to −160 mV) from 2.5 cm to 47.5 cm (Fig. 6). Although the model ORP do not agree with the measured ORP (Fig. 2), it is entirely appropriate to use the model to look at how chemical processes may occur and evolve the redox conditions over time or distance based on specific reactions with oxygen and metal sulfides among other components. The model is a means to look at how the redox conditions and associated As chemistry may evolve under different scenarios.

Another way to present the results of this model is to plot the chemical conditions as a function of space across the column at different times (Fig. 7, with spatial 'snapshots' at 170, 340, and 1020 min). Fig. 7 shows the progression of the reaction front across the column and the subsequent behavior of As species through the column. According to the model, the oxidative dissolution of pyrite/arsenopyrite, depletion of O_2, and As sorption onto newly-formed HFO via weak bonding (>(w)$FeOHAsO_4^{2-}$, >(w)$FeHAsO_4^-$,

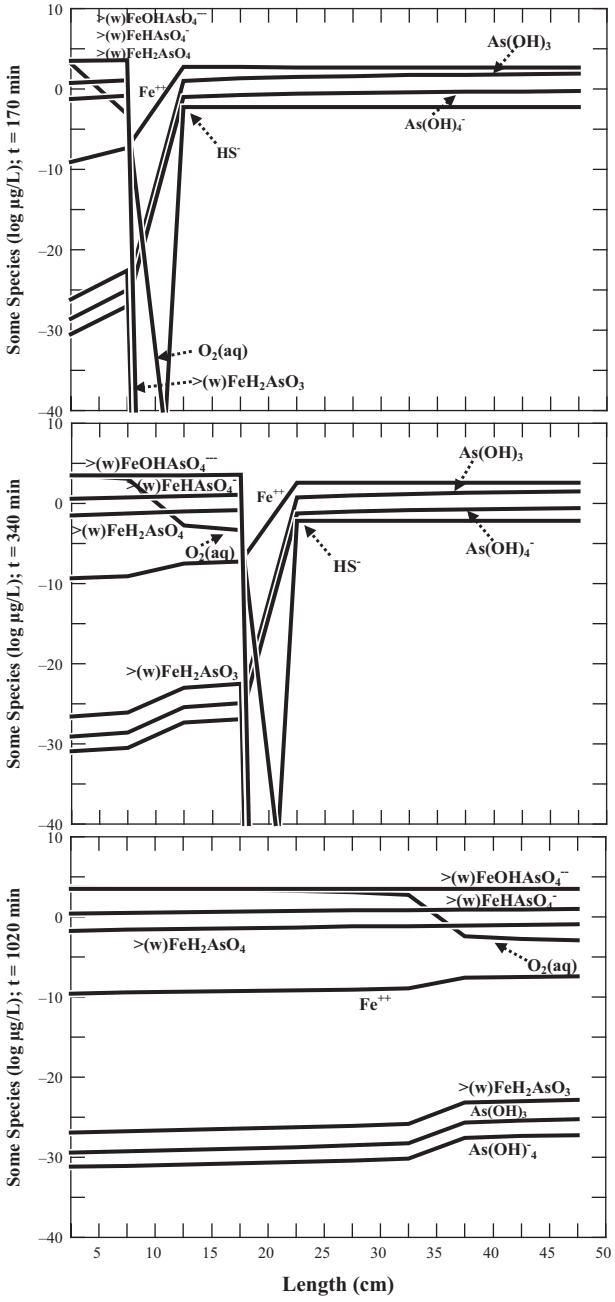

Fig. 7. Modeled distribution of As species, O_2 (aq), Fe^{2+}, and HS^- along the column at 170, 340, and 1020 min (Model 4: 1D reaction-transport model of water–rock interaction between the aquifer matrix and surface water).

>(w)FeH_2AsO_4, and >(w)FeH_2AsO_3) occurred at the reaction front, which by 340 min had moved to about 17 cm. The model showed a sharp decrease of adsorbed As and steep increase of aqueous As concentration around 22 cm at 340 min which was due the reductive dissolution of HFO (Fig. 7). This peak in As concentration is due to several processes: the coupled oxidation of pyrite containing As, As sorption to HFO, and the release of As on reduction of that same HFO. The fluid down gradient of the reaction front showed that $As(OH)_3$ and $As(OH)_4^-$ species were dominant in the column, and that the fluid was saturated with respect to pyrite, as demonstrated by the coexistence of Fe^{2+} and HS^- species (Fig. 7) (Saunders et al., 2008). Total As concentration in leachate varied from 49 μg/L (for 170 min) to 0.07 μg/L (for 1020 min). We note that the model does not account for any initial oxidation of the pyrite and formation of an oxide or sulfate salt prior to contact with oxygen in the fluid interacting with the pyrite and arsenopyrite, something that may have happened in the column experiments. The comparison of the column experiment and model results (Fig. 2 compared to Fig. 6, respectively) shows similar As levels in time but different sulfate levels in time. This suggests that the column experiment had a small amount of initial oxidation and formation of an iron–arsenic–sulfate salt from the grinding process that is unaccounted for in the model. The model (4) should be more reflective of conditions potentially occurring in calcareous aquifers.

As a modification to the model above, the discharge rate was decreased from 0.01 cm^3/cm^2 sec to 0.005 cm^3/cm^2 sec (1 mL/min), which caused the reaction front to move to 7 cm instead of about 17 cm. This change in flow rate also caused an increase in As concentration at 47.5 cm point from 36 μg/L to 49 μg/L.

4. Conclusions

Overall, the geochemical models and column experiments showed that the injection of oxidizing surface waters into reducing native groundwater cause a change in redox potential of the system and mobilization of As. The study confirmed previous work by Jones and Pichler (2007), which predicted the instability of pyrite in the Suwannee Limestone and release of As into storage-zone water, and informed the following specific conclusions:

- The column experiments suggested that As was released during injection of oxygen- and nitrate-rich surface water at concentrations higher than the current drinking water standard due to oxidative dissolution of pyrite, which was confirmed by increased pH and SO_4, and declining ORP values due to the consumption of oxygen.
- Model (1) simulated the introduction of injectate water into an aquifer under closed batch system conditions, without considering flow and no source to replenish O_2 in the fluid. It confirmed that about equivalent of 110 μg/L As was sorbed onto HFO after 300 min of the simulation, but released back to solution as $As(OH)_3$ due to the reductive dissolution of HFO. The concentration of total As in the fluid was up to 45 μg/L. The introduction of injectate water into the 0.5 m column showed that As in the first pore volume was up to 35.4 μg/L, but decreased to 23.8 μg/L after 300 min of injection.
- Model (2), modified from model (1), simulated the introduction of injectate water into an aquifer under open system conditions and to evaluate how much pyrite could react (dissolve) and to determine the amount of As, which could be leached from the aquifer matrix, if O_2 was not limited and thus conditions remained oxic. It showed that maintaining oxic conditions of the system caused the dissolution of pyrite followed by As adsorption on neo-precipitated HFO via weak bonding, resulting in only 0.4 μg/L present in the leachate.
- Model (3) simulated pyrite/arsenopyrite oxidation in an open system due to water–rock interaction between the aquifer matrix and injectate and thus, generate the corresponding release of As that was observed in the experiments. The model showed that about 0.4 g of pyrite, under the fixed molar ratio of As:FeS_2 assumed in the model, was required to dissolve from the column to achieve As concentration of 35 μg/L observed in the leaching experiments. However, those results did not agree with the amount of As observed in the native rock, and did not agree with the geochemical environment associated with ASR activities.
- 1D reaction-transport model (4) examined the results of the bench-scale experiments in time and space and evaluated the key geochemical processes occurring along the flow path. The model confirmed the assumption that a reaction front would develop and progress in the column during the injection of oxygen- and nitrate-rich water, which closely controlled the behavior of As. The processes governing the behavior of As were the oxidative dissolution of pyrite/arsenopyrite, As sorption onto newly-formed HFO via weak bonding, and the reductive dissolution of HFO causing an increase of aqueous As. The concentration of As in the leachate reached up to 36 μg/L, although it varied substantially with injection times and discharge rates.
- Models (1) and (4) were the most representative with respect to the dominant geochemical processes occurring in the columns, and supported a more complex geochemical pathway involving sulfide mineral oxidation, formation of HFO with attendant As sorption, followed by a reductive step where sorbed As is released from dissolving HFO.
- The release of As from the aquifer matrix could also be affected by a combination of additional factors outside the scope of this modeling framework. This includes changes in the porosity and permeability of the aquifer, the amount of pyrite exposed to preferential flow paths during water–rock interaction, limited surface reactivity of pyrite, favored reactions on fractured mineral surfaces, galvanic interactions between different sulfide minerals in contact, the role of As heterogeneity in individual pyrite crystals, or reactive ferrous sulfate thin films. Although these factors were not addressed in the models, they can have an influence on As mobilization.

Acknowledgments

This research was funded through a Grant from the Florida Institute of Phosphate Research and the Southwest Florida Water Management District with the assistance of Progress Energy Florida to a collaboration of Dr. Thomas Pichler and Schreuder Inc. We thank Gregg W. Jones from Cardno ENTRIX for his help with the Geochemist's Workbench and Van Deryl Wagner for his assistance in groundwater sampling on the USF Tampa campus. We are also grateful to the reviewers for their thorough and thoughtful comments that have significantly improved the manuscript.

Appendix A. Supplementary material

Supplementary data associated with this article can be found, in the online version, at http://dx.doi.org/10.1016/j.apgeochem.2014.11.006.

References

Alley, W.M., Reilly, T.E., Franke, O.L., 1999. Sustainability of Ground-Water Resources, vol. 1186. U.S. Geological Survey Circular.

Arthur, J.D., Dabous, A.A., Cowart, J.B., 2002. Mobilization of Arsenic and Other Trace Elements During Aquifer Storage and Recovery, Southwest Florida. Open-File Report 02-89, U.S. Geological Survey.

Arthur, J.D., Dabous, A.A., Cowart, J.B., 2005. Water–rock geochemical consideration for aquifer storage and recovery: Florida case studies. In: Tsang, C.F., Apps, J.A. (Eds.), Underground Injection Science and Technology, vol. 52. Developments in Water Science, Elsevier, Amsterdam, pp. 327–339.
Bethke, C.M., 2006a. The Geochemist's Workbench Release 6.0 Reaction Modeling Guide. A user's guide to React and Gtplot, University of Illinois.
Bethke, C.M., 2006b. The Geochemist's Workbench Release 6.0 Reactive Transport Modeling Guide. A user's guide to X1t, X2t, and Xtplot, University of Illinois.
Bethke, C.M., 1998. The Geochemist's Workbench Users Guide. University of Illinois.
Borda, A.M., Strongin, D.R., Schoonen, M.A., 2004. Vibrational spectroscopic study of the oxidation of pyrite by molecular oxygen. Geochimica et Cosmochimica Acta 68 (8), 1807–1813.
Bowell, R.J., 1994. Sorption of arsenic by iron oxides and oxyhydroxides in soils. Appl. Geochem. 9 (3), 279–286.
Chao, T.T., Theobald, P.K., 1976. The significance of secondary iron and manganese oxides in geochemical exploration. Econ. Geol. Bull. Soc. Econ. Geol. 71 (8), 1560–1569.
CFR (Code of Federal Regulations), 2010. Title 40, Part 144, Underground Injection Control Program.
Costagliola, P., Cipriani, C., Manganelli del Fa, C., 1997. Pyrite oxidation: protection using synthetic resins. Eur. J. Mineral. 9 (18), 167–174.
Dzombak, D.A., Morel, F.M.M., 1990. Surface Complexation Modeling: Hydrous Ferric Oxide. Wiley-Interscience, New York.
Evangelou, V.P., 1995. Pyrite Oxidation and Its Control. CRC Press, Inc., Boca Raton, pp. 293.
EPA (US Environmental Protection Agency), 2009. National Primary Drinking Water Regulations. EPA 816-F-09-0004.
Hinkle, S.R., Polette, D.J., 1999. Arsenic of the Willamette Basin, Oregon. Water-Resources Investigations Report 98-4205, Geochemistry of Arsenic, U.S. Geological Survey, pp. 28.
Hongshao, Z., Stanforth, R., 2001. Competitive adsorption of phosphate and arsenate on goethite. Environ. Sci. Technol. 35, 4753–4757.
Inskeep, W.P., McDermott, T.R., Fendorf, S., 2002. Arsenic (V)/(III) cycling in soils and natural waters: chemical and microbiological processes. In: Frankenberger, W.T., Jr. (Ed.), Environmental Chemistry of Arsenic. Marcel Dekker, Inc., pp. 183–216.
Jagucki, M.L., Katz, B.G., Crandall, C.A., Eberts, S.M., 2009. Assessing the vulnerability of public-supply wells to contamination—Floridan aquifer system near Tampa. Fact Sheet 2009–3062, U.S. Geological Survey, Florida, 6p.
Jones, G.W., Pichler, T., 2007. Relationship between pyrite stability and arsenic mobility during aquifer storage and recovery in Southwest Central Florida. Environ. Sci. Technol. 41 (3), 723–730.
Lazareva, O., Pichler, T., 2007. Naturally occurring arsenic in the Miocene Hawthorn Group, southwestern Florida: potential implication for phosphate mining. Appl. Geochem. 22, 953–973.
Manning, J.A., Goldberg, S., 1998. Adsorption and stability of arsenic (III) at the clay mineral-water interface. Environ. Sci. Technol. 31 (7), 2005–2011.
Miller, J.A., 1986. Hydrogeologic framework of the Floridan aquifer system in Florida and in parts of Georgia, South Carolina, and Alabama. Professional Paper, Report P 1403-B, U.S. Geological Survey, pp. B1–B91.
Mirecki, J.E., Bennett, M.W., Lopez-Balaez, M.C., 2012. Arsenic control during aquifer storage and recovery cycle tests in the Floridan Aquifer. Ground Water 51 (4), 539–549.
Mirecki, J.E., 2006. Geochemical Models of Water-Quality Changes During Aquifer Storage and Recovery (ASR) Cycle Tests, Phase I: Geochemical Models Using Existing Data. TR-06-8, U.S. Army Corps of Engineers, Engineers Research and Development Center.
Moses, C.O., Nordstrom, K.D., Herman, J.S., Mills, A.L., 1987. Aqueous pyrite oxidation by dissolved oxygen and by ferric iron. Geochimica et Cosmochimica Acta 51 (6), 1561–1571.
Nickson, R.T., McArthur, J.M., Ravenscroft, P., Burgess, W.G., Ahmed, K.M., 2000. Mechanism of arsenic release to groundwater, Bangladesh and West Bengal. Appl. Geochem. 15 (4), 403–413.
Pichler, T., Veizer, J., Hall, G.E.M., 1999. Natural input of arsenic into a coral-reef ecosystem by hydrothermal fluids and its removal by Fe(III) oxyhydroxides. Environ. Sci. Technol. 33 (9), 1373–1378.
Pichler, T., Price, R.E., Lazareva, O., Dippold, A., 2011. Sampling strategies for the determination of arsenic concentration and distribution in the Floridan Aquifer System. J. Geochem. Explor. 111, 84–96.
Pratesi, G., Cipriani, C., 2000. Selective depth analyses of the alteration products of bornite, chalcopyrite and pyrite performed by XPS, AES, RBS. Eur. J. Mineral. 12, 397–409.
Price, R.E., Pichler, T., 2006. Abundance and mineralogical association of arsenic in the Suwannee Limestone (Florida): implications for arsenic release during water–rock interaction. Chem. Geol. 228 (1–3), 44–56.
Saunders, J.A., Lee, M.-K., Shamsudduha, M., Dhakal, P., Uddin, A., Chowdury, M.T., Ahmed, K.M., 2008. Geochemistry and mineralogy of arsenic in (natural) anaerobic groundwaters. Appl. Geochem. 23 (11), 3205–3214.
Scott, T., 1992. A Geological Overview of Florida. Open File Report 50, Florida Geological Survey.
Stuyfzand, P.J., 1998. Quality changes upon injection into anoxic aquifers in the Netherlands: evaluation of 11 experiments. In: Peters, J.H., et al. (Eds.), Artificial Recharge of Groundwater, Rotterdam, Netherlands, Balkema, pp. 283–291.
Stuyfzand, P.J., Timmer, H., 1999. Deep Well Injection at the Langerak and Nieuwegein Sites in the Netherlands: Chemical Reactions and their Modeling. Kiwa-report SWE 96.006, Nieuwegein, Netherlands.
Vanderzalm, J.L., Dillon, P.J., Barry, K.E., Miotlinski, K., Kirby, J.K., Le Gal La Salle, C., 2011. Arsenic mobility and impact on recovered water quality during aquifer storage and recovery using reclaimed water in a carbonate aquifer. Appl. Geochem. 26, 1946–1955.
Vanderzalm, J., Dillon, P., Le Gal La Salle, C., 2007. Arsenic mobility under variable redox conditions induced during ASR. In: Fox, P. (Ed.), Management of Aquifer Recharge for Sustainability. Acadia Publishing, Phoenix, pp. 211–257.
Walker, F.P., Schreiber, M.E., Rimstidt, J.D., 2006. Kinetics of arsenopyrite oxidative dissolution by oxygen. Geochimica et Cosmochimica Acta 70, 1668–1676.
Wallis, I., Prommer, H., Pichler, T., Post, V.E.A., Norton, S., Annable, M.D., Simmons, C.T., 2011. Process-based reactive transport model to quantify arsenic mobility during aquifer storage and recovery of potable water. Environ. Sci. Technol. 45, 6924–6931.
Wallis, I., Prommer, H., Simmons, C.T., Post, V.E.A., Stuyfzand, P., 2010. Evaluation of conceptual and numerical models for arsenic mobilization and attenuation during managed aquifer recharge. Environ. Sci. Technol. 44 (13), 5035–5041.
Williams, H., Cowart, J.B., Arthur, J.D., 2002. Florida Aquifer Storage and Recovery Geochemical Study, Southwest Florida. Year One and Year Two Progress Report, Florida Geological Survey, Tallahassee, pp. 100.
Wolery et al., 1994. Thermo.dat Database Based on Data File data0.3245r46. Reformatted to Geochemist's Workbench Format as the Default. Rockware, Golden, Colorado.